

1  
2  
3  
4  
5  
6  
7  
8  
9  
10  
11  
12  
13  
14  
15  
16  
17  
18  
19  
20  
21  
22  
23  
24  
25  
26  
27

## Inverse Dynamics Modelling of Paralympic Wheelchair Curling

Brock Laschowski,<sup>1</sup> Naser Mehrabi,<sup>2</sup> and John McPhee<sup>1,2</sup>

<sup>1</sup>Department of Mechanical and Mechatronics Engineering, University of Waterloo, Canada

<sup>2</sup>Department of Systems Design Engineering, University of Waterloo, Canada

**Funding:** This research was funded by Dr. John McPhee's Tier I Canada Research Chair in Biomechatronic System Dynamics.

**Conflict of Interest Disclosure:** The authors declare that they have no conflict of interest.

**Correspondence Address:** Brock Laschowski, Department of Mechanical and Mechatronics Engineering, University of Waterloo, Ontario N2L 3G1, Canada. Email: blaschow@uwaterloo.ca. Telephone: 519-884-4567 ext. 33825

28 **Abstract**

29 Paralympic wheelchair curling is an adapted version of Olympic curling played by individuals with spinal  
30 cord injuries, cerebral palsy, multiple sclerosis, and lower extremity amputations. To the best of the  
31 authors' knowledge, there has been no experimental or computational research published regarding the  
32 biomechanics of wheelchair curling. Accordingly, the objective of this research was to quantify the angular  
33 joint kinematics and dynamics of a Paralympic wheelchair curler throughout the delivery. The angular joint  
34 kinematics of the upper extremity were experimentally measured using an inertial measurement unit  
35 system; the translational kinematics of the curling stone were additionally evaluated with optical motion  
36 capture. The experimental kinematics were numerically optimized to satisfy the kinematic constraints of a  
37 subject-specific multibody biomechanical model. The optimized kinematics were subsequently used to  
38 compute the resultant joint moments via inverse dynamics analysis. The main biomechanical demands  
39 throughout the delivery (i.e., in terms of both kinematic and dynamic variables) were about the hip and  
40 shoulder joints, followed sequentially by the elbow and wrist. The implications of these findings are  
41 discussed in relation to wheelchair curling delivery technique, musculoskeletal modelling, and forward  
42 dynamic simulations.

43

44

45

46

47

48

49

50

51

52

53 **Keywords:** multibody dynamics, biomechanical modelling, kinematic constraints, inertial measurement  
54 units, optical motion capture, sports biomechanics

## 55 **Introduction**

56 Wheelchair curling debuted at the 2006 Paralympic Games. Competing athletes utilize the same stones  
57 and ice sheets as Olympic curlers, although sweeping (i.e., using a broom to control the stone's  
58 trajectory) is omitted and the stone must be pushed from a stationary wheelchair using a delivery stick.<sup>1</sup>  
59 One of the main objectives in wheelchair curling is to launch the stone in such a way that it rectilinearly  
60 translates along the ice over 28 m and lands within the 'house' to accumulate points; this is known as a  
61 'draw shot' delivery. Research conducted at the 2010 Paralympic Games noted that 18 % of athletes  
62 competing in wheelchair curling ( $n = 50$ ) sought medical attention for musculoskeletal injuries, the  
63 majority of which were sustained about the lower back and shoulder joint.<sup>2</sup> To date, there has been no  
64 experimental or computational research published regarding the biomechanics of wheelchair curling.  
65 These investigations would provide unprecedented insights into the physical demands of this Paralympic  
66 sport.

67 One of the main objectives of biomechanists is to evaluate the dynamics (i.e., forces and  
68 moments) associated with human movements. Experimentally measuring the forces of individual skeletal  
69 muscles (i.e., dynamometry) is invasive and therefore unpractical in sport environments.<sup>3</sup> With modern  
70 advancements in computer science, biomechanical modelling presents a viable method of approximating  
71 the dynamics of multibody movements.<sup>3</sup> Considering the emergent interests in determining the physical  
72 demands of different Paralympic sports, the objectives of this research were i) to develop a subject-  
73 specific multibody biomechanical model of Paralympic wheelchair curling, and ii) to quantify the angular  
74 joint kinematics and dynamics throughout the wheelchair curling delivery via experimental measurements  
75 and inverse dynamics analysis, respectively.

## 76 **Methods**

### 77 **Paralympic Athlete**

78 A single wheelchair curler (sex: male, age: 39 y, total body mass: 87.9 kg) was recruited from the  
79 Canadian Paralympic Team. The athlete was a gold medalist at the 2014 Paralympic Games and 2013  
80 World Wheelchair Curling Championships. In 2007, the athlete sustained a traumatic incomplete spinal

81 cord injury between the 5<sup>th</sup> and 6<sup>th</sup> cervical vertebrae. The athlete was diagnosed with a level 'C'  
82 impairment on the American Spinal Injury Association Impairment Scale.<sup>4</sup> The Paralympian provided  
83 informed written consent and the University of Waterloo Research Ethics Board approved this research.

#### 84 **Experimental Kinematics**

85 The angular joint kinematics throughout the wheelchair curling delivery were experimentally measured  
86 using an inertial measurement unit (IMU) system (MVN Suit, Xsens Technologies, Netherlands). The  
87 system consists of 17 IMUs, which were attached to the Paralympian's head, torso, upper arms,  
88 forearms, hands, thighs, shanks, and feet (Figure 1). The IMU system utilises a 23-segment  
89 biomechanical model and proprietary algorithms to calculate the angular joint kinematics.<sup>5</sup> The  
90 Paralympian performed 14 'draw shot' deliveries of the curling stone interspersed with 2 minutes of rest  
91 between deliveries; all 14 deliveries were considered in the analyses. The athlete used his right hand to  
92 deliver the curling stone. Data were sampled at 120 Hz. High-frequency noise in the joint kinematic  
93 measurements was minimized using smoothing splines (MATLAB, MathWorks, USA). Previous research  
94 has demonstrated the test-retest reliability<sup>6</sup> and concurrent validity<sup>7</sup> of the IMU system in computing  
95 angular joint kinematics compared with optical motion capture.

96 Movement of the curling stone was recorded with a digital camera (Nikon D3100, Nikon  
97 Corporation, Japan) that was positioned perpendicular to the Paralympian's plane of motion. The camera  
98 sampled at 29 frames per second. The translational stone kinematics (i.e., displacements and velocities)  
99 throughout the delivery were determined relative to an inertial reference frame using markerless feature  
100 tracking software (ProAnalyst, Xcitex Incorporation, USA). The delivery is defined as the time duration  
101 between the initial displacement of the stone and its moment of release from the delivery stick. High-  
102 frequency noise in the stone kinematic measurements was minimized using smoothing splines (MATLAB,  
103 MathWorks, USA).

#### 104 **Multibody Biomechanical Model**

105 A novel biomechanical model of the wheelchair curling delivery was developed in MapleSim software  
106 (MapleSoft, Canada). The model included a representative torso, head and neck, right upper arm, right

107 forearm, right hand, delivery stick, and curling stone (Figure 2a). The wheelchair is fixed to the inertial  
 108 reference frame (Figure 2a). The mechanical parameters of each biological body segment were  
 109 experimentally measured using dual-energy x-ray absorptiometry (Table 1).<sup>8</sup> Synonymous with the  
 110 Paralympian's equipment configuration, the delivery stick body segment was set to 1.96 m in length, 0.18  
 111 kg in mass, and the principal mass moment of inertia was calculated via  $I_{zz} = \frac{1}{12}mL^2$ . The curling stone  
 112 body segment was given a mass of 19.96 kg and a height of 0.19 m.<sup>9</sup>

113 The model also included a representative hip, shoulder, elbow, and wrist, all of which were  
 114 modelled as revolute kinematic pairs (Figure 2b). The hip, shoulder, and elbow permit flexion-extension  
 115 while the wrist allows for radial-ulnar deviation, assuming a neutral hand position (Figure 2b). The hip joint  
 116 was set to 0.62 m above the inertial reference frame (i.e., simulating the height of the wheelchair seat)  
 117 (Figure 2b). The revolute joints contained angular viscous damping, the quantities of which were taken  
 118 from previous research.<sup>10-11</sup> A prismatic kinematic pair was used to model the contact between the curling  
 119 stone and ice (Figure 2b); rotations about the vertical axis were omitted. The contact model also included  
 120 dry Coulomb friction.<sup>9</sup> The multibody biomechanical model has 3 degrees of freedom and is  
 121 mathematically represented by 4 ordinary differential equations and 1 algebraic equation (i.e., indicative  
 122 of the model's kinematic constraints).

### 123 Kinematic Constraints

124 The experimental kinematics were numerically optimized to satisfy the kinematic constraints of the  
 125 multibody biomechanical model. A nonlinear constrained optimization algorithm was used to minimize the  
 126 following multi-objective function at discrete time steps (i.e.,  $t = 0 \dots 0.65$  s and  $\Delta t$  resampled = 0.001 s)

$$127 \psi_t^\dagger = \text{Arg min} \left[ \sum_{i=1}^5 w_i \left( \frac{\psi_{it} - \psi_{it}^m}{\Delta \psi_{it}^m} \right)^2 + w_6 \left( \frac{AE(\theta_{1t} \dots \theta_{4t})}{L} \right)^2 + w_7 \left( \frac{x_t - f(\theta_{1t} \dots \theta_{4t})}{\Delta x^m} \right)^2 \right] \quad (1)$$

$$128 \text{ subject to: } \psi_{min}^m < \psi_t < \psi_{max}^m \quad (2)$$

129 where  $\psi = [\theta_1 \ \theta_2 \ \theta_3 \ \theta_4 \ x]^T$ ,  $\psi^m$  represents the experimentally measured  $\psi$  variables,  $W_1 \dots W_7$  are  
 130 weighting terms (i.e.,  $W_1 = 15$ ,  $W_2 = 0.1$ ,  $W_3 = 0.95$ ,  $W_4 = 1.5$ ,  $W_5 = 200$ ,  $W_6 = 100$ , and  $W_7 = 100$ ),  $AE$   
 131  $(\theta_{1j} \dots \theta_{4j})$  is the algebraic constraint equation from the multibody biomechanical model, and  $L$  (i.e., 0.43 m)

132 is the vertical distance between the heights of the wheelchair seat and curling stone handle.  $f(\theta_1 \dots \theta_4)$   
133 denotes the modelled displacement ( $x$ ) of the curling stone in terms of the variables  $\theta_1 \dots \theta_4$ . Equation (2)  
134 specifies the minimum and maximum bounds on each  $\psi$  variable. The Paralympian's maximum range of  
135 motion about the hip ( $\theta_1$ ), shoulder ( $\theta_2$ ), elbow ( $\theta_3$ ), and wrist ( $\theta_4$ ) were experimentally measured using a  
136 digital goniometer.  $\Delta\psi$  is the difference between  $\psi_{min}^m$  and  $\psi_{max}^m$ .

### 137 Inverse Dynamics

138 Inverse dynamics is a mathematical technique through which resultant forces and moments about  
139 individual joints are calculated by solving the Newton-Euler equations of motion given the kinematics and  
140 inertial parameters of adjacent body segments.<sup>3</sup> The MapleSim software was used to solve the Newton-  
141 Euler equations of motion for the resultant joint moments about the hip, shoulder, and elbow using the  
142 optimized kinematics. The wrist was modelled as a passive joint (i.e., unactuated) in the interests of  
143 simulating the limited hand functionality of the Paralympic wheelchair curler.

### 144 Results

145 The shoulder joint displayed the largest range of motion (i.e.,  $\Delta 142.7 \pm 3.1^\circ$ ) throughout the wheelchair  
146 curling delivery compared to the hip (i.e.,  $\Delta 27.0 \pm 2.9^\circ$ ), elbow (i.e.,  $\Delta 96.7 \pm 3.3^\circ$ ), and wrist (i.e.,  $\Delta 22.8$   
147  $\pm 1.7^\circ$ ) (Figure 3). The mean duration of the delivery was approximately 0.65 seconds. The delivery was  
148 initiated through rotations about the hip (i.e., flexion), followed sequentially by the shoulder (i.e., flexion),  
149 elbow (i.e., extension), and wrist (i.e., ulnar deviation).

150 The shoulder joint had the largest magnitude of angular velocity throughout the delivery, with a  
151 maximum flexion velocity of  $427.2 \pm 12.6$  °/s and extension velocity of  $-4.1 \pm 16.4$  °/s (Figure 4). The hip  
152 joint had a maximum flexion velocity of  $-133.8 \pm 10.2$  °/s (Figure 4). The elbow joint had a maximum  
153 flexion velocity of  $21.0 \pm 13.3$  °/s and extension velocity of  $-299.7 \pm 16.7$  °/s (Figure 4). The wrist joint had  
154 a maximum radial-deviation velocity of  $17.2 \pm 9.6$  °/s and ulnar-deviation velocity of  $-126.3 \pm 12.1$  °/s  
155 (Figure 4).

156           There was minimal translational stone acceleration just before the moment of release (Figure 5);  
157 this technique is presumably used by the Paralympian to enhance precision. The translational release  
158 velocity (i.e.,  $2.0 \pm 0.1$  m/s) correlated with that reported by recent mathematical models of curling stone  
159 mechanics.<sup>9</sup> The uncertainties in the translational stone velocities slightly increased as a function of the  
160 duration of the delivery (Figure 5). The curling stone displaced a maximum of  $0.80 \pm 0.02$  m throughout  
161 the delivery (Figure 5). The Paralympian exhibited a high degree of inter-delivery consistency, as  
162 evidenced by the minor uncertainties in the stone kinematics (Figure 5).

163           The largest joint moments throughout the wheelchair curling delivery were about the hip joint (i.e.,  
164 maximum of  $203.2 \pm 34.9$  Nm), followed by the shoulder (i.e., maximum of  $54.6 \pm 6.2$  Nm) and elbow (i.e.,  
165 maximum of  $12.6 \pm 2.2$  Nm) (Figure 6).

## 166 **Discussion**

167 The objectives of this research were i) to develop a subject-specific multibody biomechanical model of  
168 Paralympic wheelchair curling, and ii) to quantify the angular joint kinematics and dynamics throughout  
169 the wheelchair curling delivery via experimental measurements and inverse dynamics analysis,  
170 respectively. The main kinematic demands throughout the delivery (i.e., in terms of maximum range of  
171 motion and angular velocity) were about the shoulder joint; this may explain why previous research found  
172 the highest incidences of musculoskeletal injuries in Paralympic wheelchair curling were about the  
173 shoulder.<sup>2</sup> The Paralympian initiated the delivery via forward hip flexion, followed sequentially by shoulder  
174 flexion, elbow extension, and ulnar-deviation. This kinematic sequencing resembles a 'follow-through'  
175 technique. The Paralympian's delivery technique was also highly reproducible, as evidenced by the minor  
176 uncertainties in the joint (Figures 3-4) and stone (Figure 5) kinematics. To the best of the authors'  
177 knowledge, these findings represent the first documented kinematic analysis of the wheelchair curling  
178 delivery. Although the joint kinematics might be considered indicative of an 'optimal' delivery technique  
179 (i.e., since the athlete is a Paralympic gold medalist), additional research is needed to ascertain the  
180 delivery kinematics of other Paralympic wheelchair curlers to derive statistically significant conclusions.

181           The multibody biomechanical model was used to evaluate the resultant joint moments about the  
182 lower back and upper extremity joints throughout the wheelchair curling delivery. Resultant joint moments  
183 are mathematical summations of the dynamics from all neighbouring biological elements (e.g., skeletal  
184 muscles, tendons, ligaments, and bursae).<sup>3</sup> Consequently, the forces and moments from individual  
185 skeletal muscles cannot be determined. For example, the positive resultant joint moment about the elbow  
186 joint throughout the wheelchair curling delivery (Figure 6) could be attributed to either activations of the  
187 agonist muscles (e.g., biceps brachii) or deactivations of the antagonist muscles (e.g., triceps brachii).  
188 Musculoskeletal models would be needed to evaluate the activations and dynamics of individual skeletal  
189 muscles throughout the wheelchair curling delivery. These models could provide further insights into the  
190 documented musculoskeletal injuries amongst Paralympic wheelchair curlers.<sup>2</sup>

191           Considering a wide variety of individuals with physical disabilities compete in wheelchair curling,  
192 including those with spinal cord injuries, cerebral palsy, multiple sclerosis, and lower extremity  
193 amputations,<sup>1</sup> it is important to quantify the maximum physical demands associated with the delivery  
194 movement. The resultant joint moments throughout the wheelchair curling delivery were calculated using  
195 inverse dynamics analysis. The maximum dynamic loads were computed about the hip joint, followed  
196 sequentially by the shoulder and elbow. Nevertheless, inverse dynamics is not predictive, and requires  
197 expensive and time-consuming experiments. Forward dynamics, by contrast, computes the multibody  
198 kinematics by numerically integrating the Newton-Euler equations of motion given the forces and  
199 moments as inputs; these dynamic inputs are often elicited from mathematical models of neural  
200 excitations.<sup>3</sup> Forward dynamics has the distinct capability of i) predicting the effects of model parameters  
201 (e.g., height of the wheelchair seat) on performance outcomes, and ii) optimizing equipment designs *in*  
202 *silico*.<sup>12</sup> Consequently, the authors intend to further investigate the biomechanics of wheelchair curling  
203 using forward dynamic simulations.



204 **Acknowledgments**

205 The authors thank the Paralympic wheelchair curler for participating in this research. The authors also  
206 recognize the Canadian Sport Institute Ontario and Curling Canada for their support. This research was  
207 funded by Dr. John McPhee's Tier I Canada Research Chair in Biomechatronic System Dynamics.

208 **Conflict of Interest**

209 The authors declare that they have no conflict of interest.

ACCEPTED

210 **References**

- 211 1. World Curling Federation. The Rules of Curling and Rules of Competition.  
212 <http://www.worldcurling.org/rules-and-regulations>. Published October 2015. Accessed May 2016.
- 213 2. Webborn N, Willick S, Emery CA. The injury experience at the 2010 Winter Paralympic Games. *Clinical*  
214 *Journal of Sports Medicine*. 2012;22:3-9.
- 215 3. Roberston DGE, Caldwell GE, Hamill J, Kamen G, Whittlesey SN. *Research Methods in Biomechanics*.  
216 2nd ed. Champaign, USA: Human Kinetics; 2014.
- 217 4. Kirshblum SC et al. International standards for neurological classification of spinal cord injury (Revised  
218 2011). *Journal of Spinal Cord Medicine*. 2011;34:535-546.
- 219 5. Roetenberg D. *Inertial and Magnetic Sensing of Human Motion*. [PhD Dissertation]. Enschede, The  
220 Netherlands: University of Twente; 2006.
- 221 6. Cloete T, Scheffer C. Repeatability of an off-the-shelf, full body inertial motion capture system during  
222 clinical gait analysis. *Proceedings of the IEEE 32<sup>nd</sup> Annual International Conference of the Engineering in*  
223 *Medicine and Biology Society*. 2010: 5125-5128.
- 224 7. Zhang JT, Novak AC, Brouwer B, Li Q. Concurrent validation of Xsens MVN measurement of lower  
225 limb joint angular kinematics. *Physiological Measurement*. 2013;34:63-69.
- 226 8. Laschowski B, McPhee J. Body segment parameters of Paralympic athletes from dual-energy X-ray  
227 absorptiometry. *Sports Engineering*. 2016;19:155-162.
- 228 9. Maeno N. Dynamics and curl ratio of a curling stone. *Sports Engineering*. 2014;17:33-41.
- 229 10. Lebedowska MK. Dynamic properties of human limb segments. In: Karwowski W, ed. *International*  
230 *Encyclopaedia of Ergonomics and Human Factors*. 2nd ed. Boca Raton, USA: CRC Press; 2006:315-  
231 319.

- 232 11. Rapoport S, Mizrahi J, Kimmel E, Verbitsky O, Isakov E. Constant and variable stiffness and damping  
233 of the leg joints in human hopping. *Journal of Biomechanical Engineering*. 2003;125:507-514.
- 234 12. Balzerson D, Banerjee J, McPhee J. A three-dimensional forward dynamic model of the golf swing  
235 optimized for ball carry distance. *Sports Engineering*. 2016. doi:10.1007/s12283- 016-0197-7.

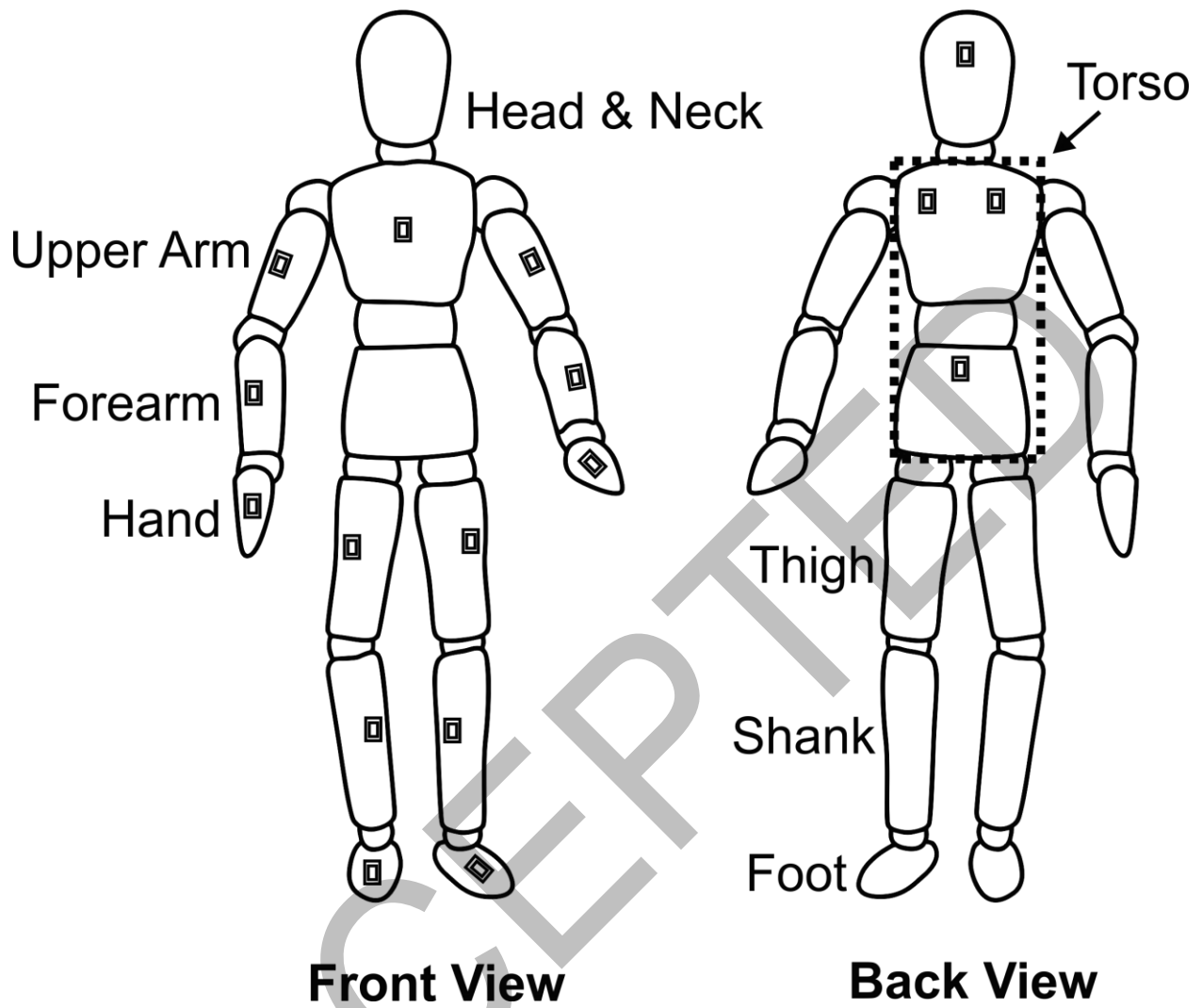
ACCEPTED

236 **Table 1.** Body segment parameters of the Paralympic wheelchair curler as experimentally measured  
237 using dual-energy x-ray absorptiometry.<sup>8</sup> The quantities are presented as arithmetic means  $\pm$  1 standard  
238 deviation over multiple scans. Segments in the upper extremity are of the right side. The position vector of  
239 the center of mass was determined relative to the proximal endpoint.

Parameter	Head & Neck	Torso	Upper Arm	Forearm	Hand
Length (m)	0.265 $\pm$ 0.005	0.588 $\pm$ 0.008	0.291 $\pm$ 0.005	0.276 $\pm$ 0.002	0.123 $\pm$ 0.002
Mass (kg)	6.967 $\pm$ 0.085	44.616 $\pm$ 0.677	3.099 $\pm$ 0.192	1.371 $\pm$ 0.009	0.396 $\pm$ 0.011
Center of Mass (m)	0.1231 $\pm$ 0.0025	0.2237 $\pm$ 0.0031	0.149 $\pm$ 0.002	0.108 $\pm$ 0.001	0.022 $\pm$ 0.001
Mass Moment of Inertia (kg·m <sup>2</sup> )	0.1963 $\pm$ 0.0102	2.8508 $\pm$ 0.0349	0.0238 $\pm$ 0.0022	0.0106 $\pm$ 0.0002	0.0022 $\pm$ 0.0001

240

241



242

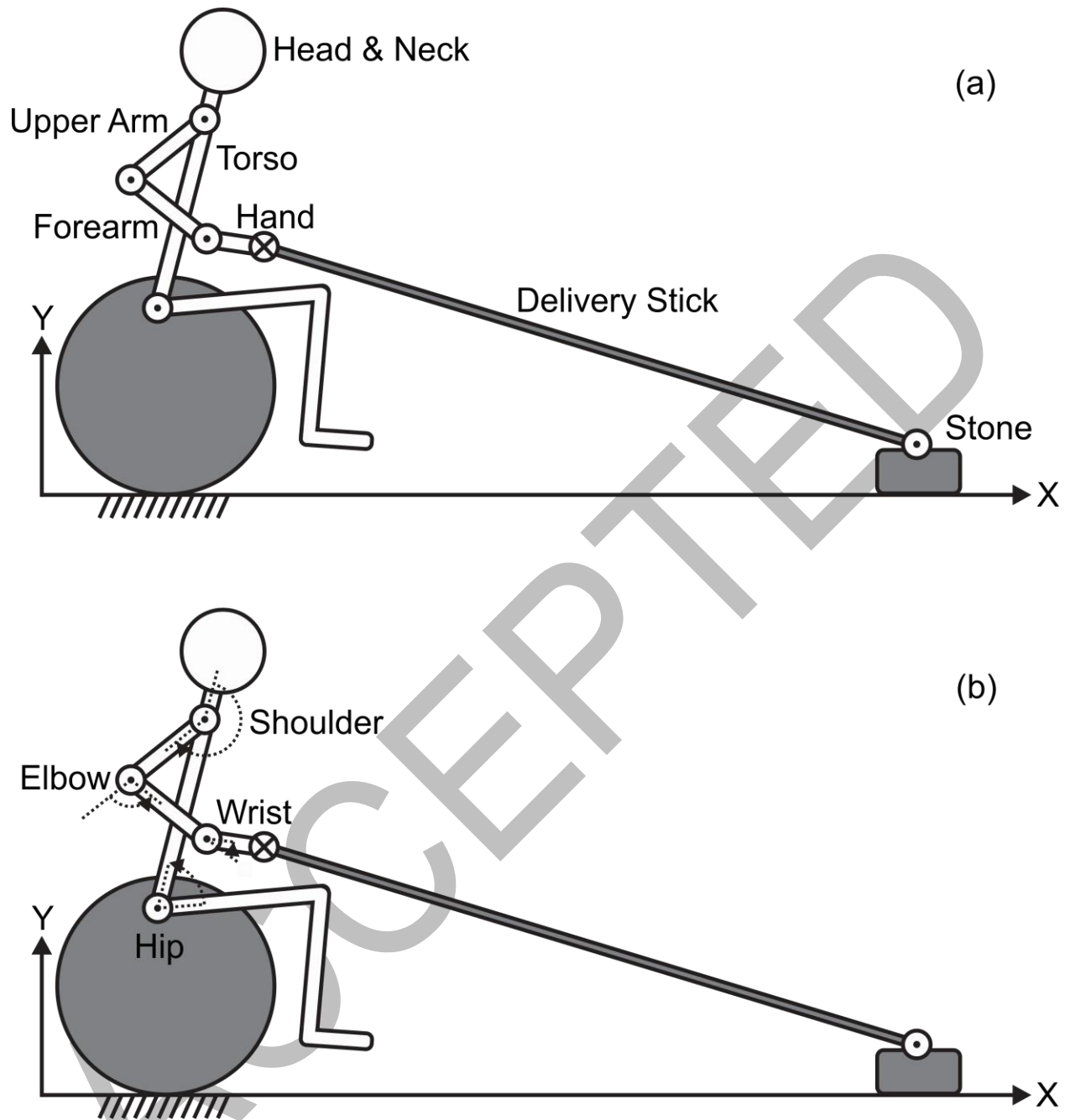
243

244

**Figure 1** – Locations of the inertial measurement units on the Paralympic wheelchair curler.

245

246



247

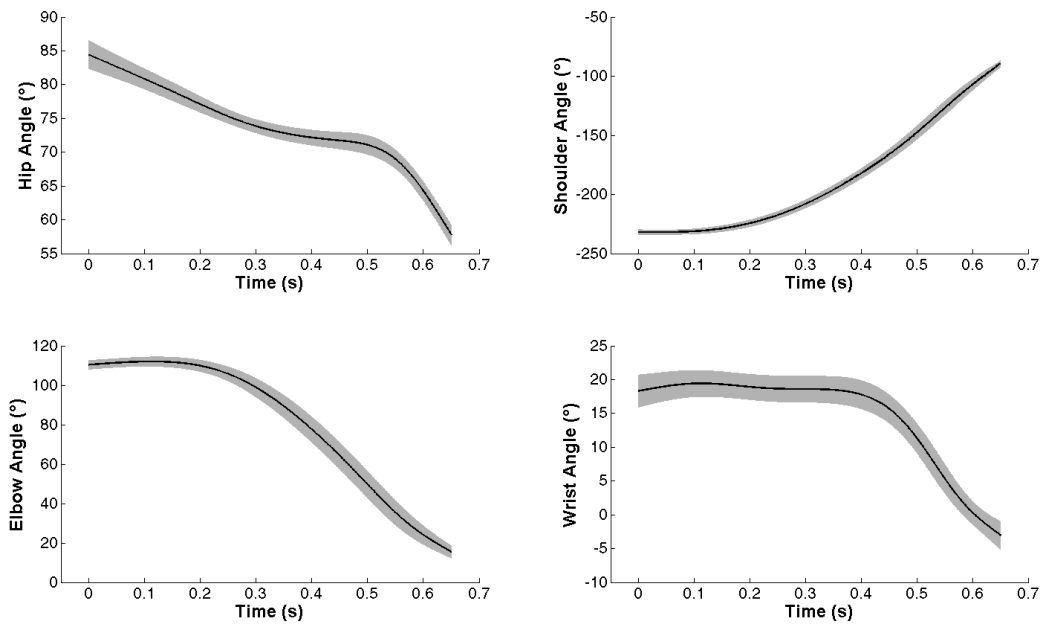
248

249 **Figure 2** - Schematic of the multibody biomechanical model. The rigid body segments and lower

250 kinematic pairs are presented in (a) and (b), respectively.

251

252



253

254

255

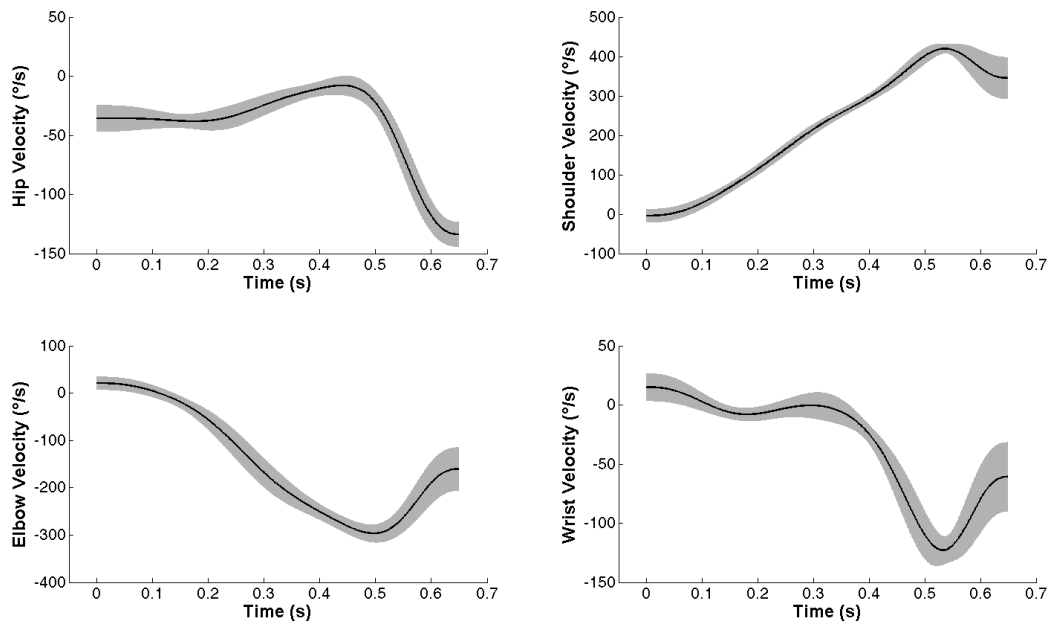
256

257

258

259

**Figure 3** - The relative joint angles of the hip, shoulder, elbow, and wrist throughout the wheelchair curling delivery. The quantities are presented as arithmetic means  $\pm$  1 standard deviation over 14 consecutive deliveries.



260

261

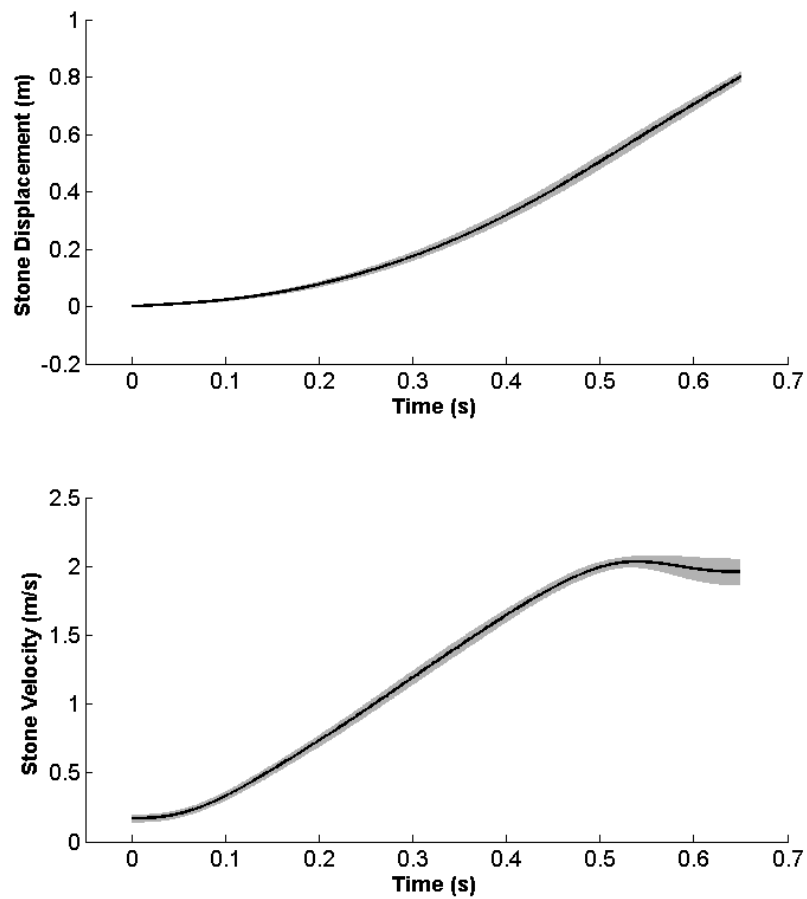
262 **Figure 4** - The angular joint velocities of the hip, shoulder, elbow, and wrist throughout the wheelchair

263 curling delivery. The quantities are presented as arithmetic means  $\pm$  1 standard deviation over 14

264 consecutive deliveries.

265

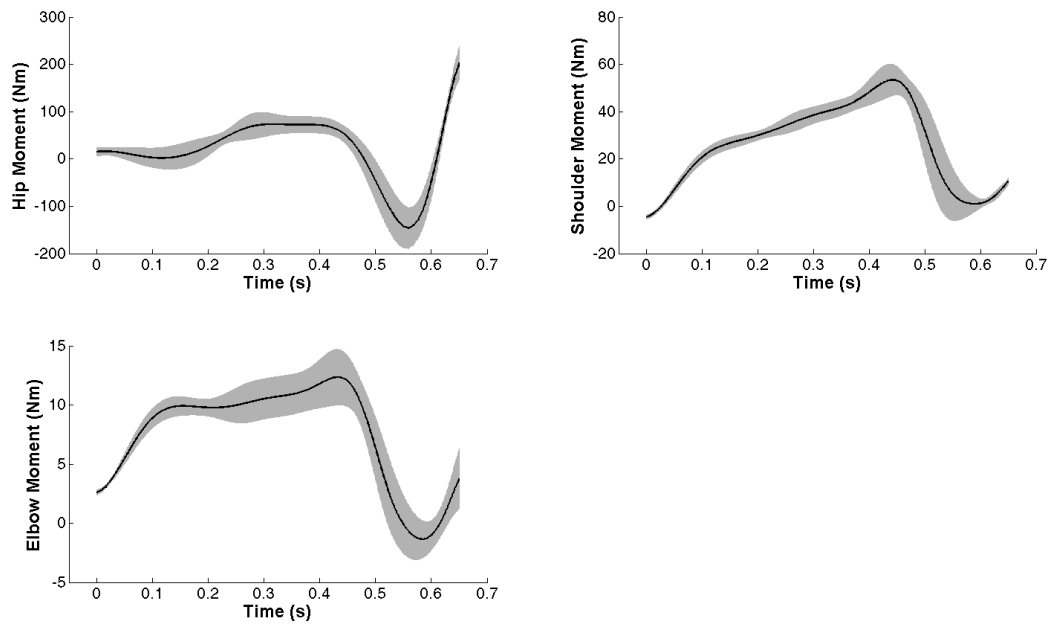




266

267 **Figure 5** - The translational stone kinematics (i.e., displacements and velocities) throughout the  
268 wheelchair curling delivery. The quantities are presented as arithmetic means  $\pm$  1 standard deviation over  
269 14 consecutive deliveries.

270



271

272

273

274

275

**Figure 6** - The resultant joint moments about the hip, shoulder, and elbow as computed via inverse dynamics analysis. The quantities are presented as arithmetic means  $\pm$  1 standard deviation over 14 consecutive deliveries.